

# Micelles-in-Liposome Systems Obtained by Proliposomal Approach for Cannabidiol Delivery: Structural Features and Skin Penetration

Silvia Franzè,\* Caterina Ricci, Elena Del Favero, Francesco Rama, Antonella Casiraghi, and Francesco Cilurzo



Cite This: <https://doi.org/10.1021/acs.molpharmaceut.3c00044>



Read Online

ACCESS |



Metrics & More



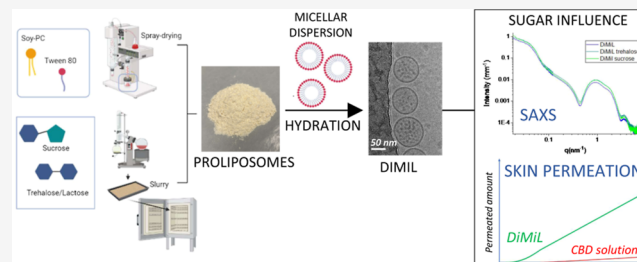
Article Recommendations



Supporting Information

**ABSTRACT:** Deformable liposomes represent valuable drug carriers for cutaneous administration. Nevertheless, the fluid lipid membrane can favor the drug leakage during storage. Proliposomes may represent a suitable strategy to solve this issue. As an alternative, a novel carrier, which encloses hydrophobic drugs in the inner core of vesicles, namely, a drug-in-micelles-in-liposome system (DiMiL), has been proposed. In this work, we investigated the possible advantages of combining these two approaches to obtain a formulation able to enhance the skin penetration of cannabidiol (CBD). Proliposomes were prepared by spray-drying or slurry method testing lactose, sucrose, and trehalose as carriers at different sugar/lipid weight ratios. The ratio between soy phosphatidylcholine (main lipid) and Tween 80 was instead fixed at 85:15 w/w. DiMiL systems were extemporaneously obtained by the hydration of proliposomes with a Kolliphor HS 15 micellar dispersion (containing CBD, when appropriate). Based on the technological properties, sucrose and trehalose at 2:1 sugar/lipid ratio resulted in the best carriers for spray-dried and “slurried” proliposomes, respectively. Cryo-EM images clearly showed the presence of micelles in the aqueous core of lipid vesicles and the presence of sugars did not alter the structural organization of DiMiL systems, as demonstrated by SAXS analyses. All formulations were highly deformable and able to control CBD release regardless of the presence of sugar. The permeation through human epidermis of CBD carried by DiMiL systems was significantly improved if compared to that obtained loading the drug in conventional deformable liposomes with the same lipid composition or in an oil solution. Furthermore, the presence of trehalose led to a further slight increase of the flux. Altogether, these results demonstrated that proliposomes may be a valuable intermediate for the preparation of deformable liposome-based cutaneous dosage forms, improving the stability without compromising the overall performances.

**KEYWORDS:** proliposomes, deformable liposomes, cannabidiol, trehalose, SAXS, skin penetration



## 1. INTRODUCTION

The skin is an excellent barrier evolved to protect the body from the external environment. In particular, the outermost layer of the skin, the stratum corneum, is responsible for this function thanks to its complex and particular organization, being composed of several layers of overlapped dead cells, namely, the corneocytes, embedded in a lipid matrix. This so-called “brick and mortars” structure prevents the passive diffusion of xenobiotics, including most of the active ingredients applied on the skin. This is the reason why still today (trans)dermal administration is limited to very few compounds with unique physico-chemical properties. These are mainly low molecular weight (<500 Da), oil/water partition coefficient ranging from 1 to 3, a certain solubility both in oil and in water and, when a systemic effect is desired, a low daily dose.<sup>1</sup>

Several strategies have been developed to breach the skin barrier and one of the most studied is the use of nanotechnology and in particular, deformable liposomes.

These are lipid vesicles that seem to be able to undergo a reversible deformation under stress to pass through the nanosized pores (20–40 nm) physiologically present among corneocytes, thus delivering the cargoes in the deeper layers of the skin.<sup>2,3</sup> This behavior is ascribed to the composition of these vesicles that are appositely designed to have a very fluid membrane. For this reason, deformable liposomes are generally composed of lipids with a very low transition temperature (lower than 25 °C), they do not contain stabilizing agents such as cholesterol, but instead contain some softening agents, namely, compounds that, sitting in the bilayer or coming into contact with it, decrease the Young modulus of the vesicles.<sup>57</sup>

**Received:** January 18, 2023

**Revised:** June 1, 2023

**Accepted:** June 1, 2023

58 Examples of softening agents are single chain surfactants and  
59 ethanol.<sup>4</sup> Deformable liposomes have been demonstrated to  
60 improve the skin penetration of several compounds regardless  
61 of the physico-chemical characteristics.<sup>5,6</sup> Nevertheless, the  
62 fluid membrane of deformable liposomes may be responsible  
63 for instability phenomena decreasing the shelf-life of the  
64 product and then the possibility to reach the market. The main  
65 stability issue relies on the easier diffusion of loaded drugs  
66 through the leaky membranes that, depending on the strength  
67 of the affinity between drug and lipids, can result in a great  
68 extent of drug leakage.<sup>7</sup>

69 Proliposomes are provesicular products that can be  
70 successfully exploited to overcome these instability issues.  
71 The production of proliposomes involves the coating of  
72 phospholipids on a soluble carrier with high surface area and  
73 porosity (e.g., sugars) to form a dry powder that effectively  
74 forms liposomes upon contact with water.<sup>8</sup> Although the  
75 proliposome approach has been proposed several years ago,  
76 less than 250 papers dealing with the design of proliposomes  
77 can be found in literature and many of them are related to the  
78 development of dry powders for inhalation or oral solid dosage  
79 forms. Very few data are available on the design of  
80 proliposomes to be applied on the skin, either in the form of  
81 powders (to be converted into liposomes directly after contact  
82 with the skin moisture)<sup>9</sup> or after loading in semisolid  
83 preparations, such as gels and creams.<sup>10,13</sup> Moreover, none of  
84 the previous works reported the use of proliposomes as  
85 precursors of deformable liposomes and, therefore, a system-  
86 atic study on the impact of the production method and  
87 selected excipients on the properties of these final vesicles (e.g.,  
88 deformability) is missing. This lack of information limited the  
89 possibility to identify a consistent formulation space and the  
90 critical quality attributes required for the design and develop-  
91 ment of an optimal formulation.

92 An alternative approach to limit the drug leakage while  
93 maintaining deformable liposomes in aqueous dispersion is the  
94 use of DiMiL, a novel carrier recently proposed, which is  
95 basically a dual carrier in which hydrophobic drugs are  
96 encapsulated in the aqueous core of the liposomes through  
97 micellar solubilization. With this expedient the concentration  
98 gradient of the free drug is decreased, limiting the drug leakage  
99 phenomenon. Along with the better stability, the DiMiL  
100 system was demonstrated to have greater efficiency in  
101 enhancing the permeation of poorly permeable compounds  
102 through human skin with respect to “conventional” deformable  
103 liposomes with a similar lipid composition.<sup>14</sup>

104 To facilitate the industrial production and further improve  
105 the stability over time of deformable liposomes, in this work  
106 the feasibility to prepare DiMiL systems by proliposome  
107 approach was investigated, studying the effect of the  
108 manufacturing process and excipients choice on the techno-  
109 logical (i.e., vesicle deformability) and biopharmaceutical  
110 properties (i.e., drug release and drug skin permeation) of  
111 DiMiL. The attention was focused mainly on the role of sugar  
112 carriers on the structure and skin permeation performances of  
113 DiMiL systems, also considering the fact that sugars, such as  
114 trehalose, might have a skin hydration effect that can in turn  
115 change the overall skin penetration behavior of the system.<sup>15</sup>

116 Proliposomes were prepared by both spray-drying and slurry  
117 method,<sup>16,17</sup> testing three different carriers, namely, lactose,  
118 sucrose, and trehalose, at different weight ratios with respect to  
119 phospholipid, namely, soy-phosphatidylcholine (s-PC). DiMiL  
120 systems obtained following the hydration with the micellar

dispersion of the prepared proliposomal powders (*p*-DiMiL) 121  
were then characterized for their main physico-chemical 122  
properties (i.e., particle size distribution and deformability), 123  
in comparison with analogous formulations prepared by 124  
conventional methods (i.e., thin lipid film hydration method) 125  
and, therefore, differing only for the presence of the carrier. 126  
Details on the structure and on the internal arrangement of 127  
components were obtained by cryo-EM and small-angle X-ray 128  
scattering (SAXS). The latter technique can provide important 129  
and novel information on the DiMiL ultrastructure, meanwhile 130  
clarifying the role of micelle concentration and sugars on the 131  
particular micelles-in-liposome organization. The skin pene- 132  
tration performances were assessed using cannabidiol (CBD) 133  
selected as the growing interest in inflammation-based skin 134  
diseases.<sup>18,19</sup> 135

## 2. MATERIALS AND METHODS

**2.1. Materials.** Soy-phosphatidylcholine (s-PC) and 1,2- 136  
dipalmitoyl-*sn*-glycero-3-phosphocholine (DPPC) were kindly 137  
provided by Lipoid (Steinhausen, Switzerland); Kolliphor HS 138  
15 (critical micellar concentration in the 0.005–0.02% range) 139  
was provided by BASF (Cesano Maderno, Italy); Tween 80 140  
(T80) was purchased from Croda Chocques (France); vaseline 141  
oil, trehalose dihydrate, and ascorbic acid were obtained from 142  
VWR International (I); and ammonium molybdate, sodium 143  
dihydrogen phosphate, lactose, sucrose, and analytical-grade 144  
organic solvents were obtained from Merck Life Science 145  
(Milan, Italy). Cannabidiol (CBD) was kindly gifted by Indena 146  
(Italy). 147

**2.2. Preparation of Proliposomes.** Proliposomes were 148  
composed of s-PC and T80 in weight ratio of 85:15; trehalose, 149  
sucrose, or lactose were added in sugar/lipid weight ratio 150  
ranging from 1:1 to 1:3. Powder formulations were obtained 151  
by the following methods: 152

Spray-drying (SD)—the main formulative and process 153  
variables were studied to obtain powders from feeds containing 154  
at least 10% w/w solid, having a water content lower than 5%, 155  
a yield higher than 80% and in which the main chemical status 156  
of lipids was preserved. The feeds were prepared by 157  
suspending the sugar in the lipid organic solutions or dissolving 158  
the sugar and the lipid components in water/organic solvent 159  
mixtures. In particular, different solvents miscible with water 160  
(i.e., ethanol and methanol) as well as different concentrations 161  
of the components were screened. 162

Feeds were spray-dried by a 4M8 spray-drier (Procept, 163  
Netherlands) equipped with a 0.6 mm nozzle with an inlet 164  
temperature of 150 °C (measured chamber temperature: 57° 165  
± 1 °C) and a feed flux of 10 mL/min. 166

Slurry method (SL)—initially, sugars were micronized to 167  
increase the surface area using an ultra-centrifugal mill (Ultra 168  
Centrifugal Mill ZM 200, Retsch, Germany) equipped with a 169  
120 μm mesh size sieve. Samples were mixed with dry ice in 170  
the mill hopper and rotor speed was fixed at 6000 rpm. 171

For the preparation of proliposomes, s-PC and Tween 80 172  
were dissolved in ethyl acetate in a 100 mL round-bottom 173  
flask. After adding the micronized carrier to reach a final solid 174  
content of 12% w/v, the solvent was mostly evaporated at 40 175  
°C under reduced pressure by using a rotary evaporator HB10 176  
(IKA, Germany), and then, the slurry was completely dried at 177  
70 °C overnight. The resulting dry powder was collected and 178  
the granulometry was uniformed by sieving the powder 179  
through a 355 μm sieve. 180

Table 1. Composition and Main Characteristics of DiMiL Systems<sup>a</sup>

form. code	micelle content (% w/v)	sPC/sugar ratio	sugar	D (nm)	PdI	K (mN/mm)	EE %
S1	10	1/1	sucrose	118	0.4	10 ± 2	
S1.5	10	1/1.5	sucrose	109	0.3	10 ± 3	
S2	10	1/2	sucrose	108	0.3	10 ± 2	
S3	10	1/3	sucrose	117	0.3	13 ± 3	
S2-C	10	1/2	sucrose	95	0.3	1 ± 0	49.4 ± 4.8
T2	10	1/2	trehalose	112	0.3	11 ± 4	
T3	10	1/3	trehalose	129	0.3	9 ± 2	
T2-C	10	1/2	trehalose	129	0.3	4 ± 3	45.5 ± 2.4
FH0				117	0.1	8 ± 1	
FH4	4			122	0.1	2 ± 1	
FH10	10			125	0.1	7 ± 3	
FH0-C				106	0.1	3 ± 0	52.8 ± 3.0
FH4-C	4			138	0.2	5 ± 1	35.8 ± 1.2
FH10-C	10			140	0.2	2 ± 0	45.8 ± 1.3

<sup>a</sup>FH: liposomes prepared by the thin lipid film hydration method; S: sucrose (spray-drying method); T: trehalose (slurry method); and C/CBD. The standard deviation on *D* is lower than 1 nm, on the PDI is lower than 0.05.

**2.3. Preparation of DiMiL Formulations.** Blank DiMiL formulation was obtained by hydrating proliposomal powders with a 4 or 10% w/v Kolliphor micellar dispersion for 1 h at 40 °C using an overhead paddle stirrer at 350 rpm (RW-20, DZM Jankel & Kunkel, Germany). In case of drug-loaded formulations, CBD at the concentration of 3.5 mg/mL was preliminarily loaded in micelles and then CBD micellar dispersion was used as hydration medium. Particle size was uniformed by 5 min sonication (30 s on and 30 s off) using a probe sonicator UP200St (Hielscher, Germany). The formulation composition is summarized in Table 1.

In both cases, DiMiL were purified by un-entrapped micelles by size-exclusion chromatography using Sepharose-4CL columns and eluting with ultrapure water.

As the control, DiMiL systems were also prepared by the conventional thin lipid film hydration method (FH-formulations, Table 1).<sup>14</sup> The final concentration of bilayer components was set at 30 mg/mL for all formulations independently of the preparation method.

**2.4. Characterization of Proliposomes.** In the first instance, proliposomal powders were analyzed in terms of granulometry, water content, and flowability. The granulometry was assessed directly on the dry proliposomal powders using the laser diffraction particle size analyzer Mastersizer 3000 (Malvern, UK).

The moisture content (MC) was measured by a Volumetric Karl Fischer titration V20 (Mettler Toledo, Italy). Samples were prepared by dissolving 10 mg of proliposomes in 1 mL of anhydrous methanol. Afterward, samples of 500 μL of methanol were injected into the titration vessel. The water content was measured in triplicate.

Powder flowability was assessed by measuring the angle of repose and the compressibility index according to the European Pharmacopeia. To assess the angle of repose, about 5 g of powder was allowed to drain from a funnel of 12 mm with a height of 5 cm from the plane basis. The angle of repose ( $\alpha$ ) was calculated according to the following equation

$$\tan(\alpha) = \frac{\text{height}}{0.5 \times \text{base}}$$

To assess the compressibility index ( $I_c$ ), about 100 g of powder was put in a 250 mL volumetric cylinder and tapped 100 times.  $I_c$  was calculated as follows

$$I_c = 100 \times \frac{V_0 - V_f}{V_0}$$

where  $V_0$  is the unsettled apparent volume and  $V_f$  is the final tapped volume.

Finally, phospholipid oxidation in proliposomal powders was studied according to the method described by Goldbach et al.<sup>20</sup> Briefly, raw s-PC and proliposomes were dissolved in absolute ethanol to get the s-PC concentration of 1 mg/mL. The absorbance values measured at 215 and 233 nm (Lambda 25, PerkinElmer—USA) were used to calculate the oxidation index (*R*) as the ratio  $A_{233\text{nm}}/A_{215\text{nm}}$ .

**2.5. Characterization of DiMiL System.** **2.5.1. Physico-Chemical Characterization.** DiMiL systems obtained after re-hydration of the proliposomal powders with Kolliphor dispersions were characterized in terms of particle size distribution and  $\zeta$ -potential by dynamic light scattering (DLS) by using Nano-ZS Zetasizer (Malvern Instrument, UK). Particle size measurements were carried out by inserting the sample in a disposable cuvette after a 1:10 dilution in 0.22 μm filtered MilliQ water, with a detection angle of 173° for Zetasizer analyses. For  $\zeta$ -potential determination, the samples were inserted in a capillary cell after 1:10 dilution. Three measurements were taken for each sample and the results were expressed as the mean and standard deviation.

Encapsulation efficiency (EE, %) was determined on purified lipid vesicles after breakage of the vesicles in methanol. The quantification of CBD was carried out by using a HPLC system equipped with a diode array detector (HPLC HP 1100 Chemstations, Agilent Technologies, Germany). CBD concentration was determined by using a C8 column (150 × 4.6 mm, 5 μm; PhenoSphere-NEXTTM, Phenomenex) with a mixture of pH = 3 phosphate buffer and acetonitrile in the ratio 75/25 v/v as mobile phase. The flux was fixed at 1.5 mL/min and wavelength at 215 nm. Analyses were performed at 25 °C and the injection volume was 20 μL.<sup>11,12</sup>

**2.5.2. Determination of the Deformability Constant (*k*).** The lipid concentration of the selected formulations was measured using an adaptation of the Rouser method, as described elsewhere<sup>21</sup> and formulations were diluted to a total lipid concentration of 0.23 mM. The deformability was studied by using a dynamometer-assisted extrusion assay, previously developed.<sup>22</sup> An aliquot of 1 mL liposome dispersion was

261 loaded in a gas tight syringe which was inserted in an extruder  
262 casing and put in contact with a 50 N load cell of a  
263 dynamometer (INSTRON 5965, ITW Test and Measurement  
264 Italia Srl, Italy). The syringe plunger was moved at a constant  
265 speed of 1 mm/s, forcing the liposomal dispersion through a  
266 50 nm polycarbonate membrane fixed in the extruder casing.  
267 The resistance opposed to the passage of liposomes through  
268 the membrane was registered by the load cell and the force  
269 values (mN) were plotted versus the plunger displacement  
270 (mm). The constant of deformability ( $k$ ) was calculated as the  
271 slope of the linear part of the plot. The higher the  $k$  value, the  
272 lower the deformability of liposomes. The assay was carried  
273 out at least on three different samples for each formulation.

274 **2.5.3. Structural Characterization.** **2.5.3.1. Cryo-EM.**  
275 Sample vitrification was carried out with a Mark IV Vitrobot  
276 (Thermo Fisher Scientific). An aliquot of 4  $\mu$ L sample was  
277 applied to a Quantifoil R2/1 Cu 300-mesh grid previously  
278 glow-discharged at 30 mA for 30" in a GloQube (Quorum  
279 Technologies). Immediately after sample application, the grids  
280 were blotted in a chamber at 4 °C and 100% humidity and  
281 then plunge-frozen into liquid ethane.

282 Vitrified grids were transferred to a Talos Arctica (Thermo  
283 Fisher Scientific) operated at 200 kV and equipped with a  
284 Falcon 3 direct electron detector (Thermo Fisher Scientific).  
285 Micrographs were acquired at a nominal magnification of  
286 73'000 $\times$ , corresponding to a pixel size of 1.43 Å/pixel, in linear  
287 mode, with a defocus of  $-3.0 \mu\text{m}$  and with a total dose of 40  
288  $\text{e}^-/\text{Å}^2$ .

289 **2.5.3.2. Small-Angle X-ray Scattering.** Experiments were  
290 carried out at the ID02 beamline at ESRF (Grenoble, F) (DOI  
291 10.15151/ESRF-ES-653835676). Liposome dispersions and  
292 reference solvents were put in 2 mm capillaries (ENKI, Italy)  
293 mounted on a horizontal sample holder to be irradiated by a  
294 monochromatic X-ray beam ( $\lambda = 0.995 \text{ nm}$ ). The scattered  
295 intensity was collected on a 2D detector at two different  
296 sample-to-detector distances (1 m and 10 m) to investigate a  
297 wide range of  $q = 4\pi\sin(\theta/2)/\lambda$ , where  $\theta$  is the scattering  
298 angle. After angular regrouping and careful background  
299 subtraction, the intensity profiles  $I(q)$  give information on  
300 the structural properties of the liposomes on different length  
301 scales, from the hundreds of nms (mesoscale) to the nms  
302 (local scale). For micellar systems, the profiles were  
303 reconstructed with the SasView application (version 4.2.0,  
304 2019).

305 **2.5.4. Differential Scanning Calorimetry.** Thermal analyses  
306 were performed using a differential scanning calorimetry  
307 (DSC) 1 Stare System (Mettler Toledo, Novate Milanese,  
308 Italy), equipped with an intracooler. Samples of 40  $\mu$ L of  
309 liposome dispersions were sealed in a pin holed aluminum pan  
310 and subject to a cooling cycle from 25 to 0 °C at a cooling rate  
311 of 1 K  $\text{min}^{-1}$  and after 5 min at 0 °C, samples were heated up  
312 to 60 °C at a heating rate of 2 K  $\text{min}^{-1}$ . The DSC cell was  
313 purged with dry nitrogen at 80 mL/min.

314 **2.6. In Vitro Drug Release and Skin Permeability**  
315 **Studies.** The in vitro drug release and skin permeability  
316 studies were carried out using the Franz diffusion cells with a  
317 receiving volume of about 3.0 mL and a surface area of 0.636  
318  $\text{cm}^2$ . The drug release of CBD from selected formulations was  
319 studied as detailed elsewhere<sup>23</sup> by using an artificial membrane  
320 of nitrate cellulose.

321 The skin permeability studies were carried out using human  
322 epidermis obtained from healthy volunteers undergoing  
323 abdominoplasty and prepared according to an internal

procedure.<sup>24</sup> Briefly, the excess of fat was carefully removed 324  
and full-thickness skin is cut into squares, sealed in evacuated 325  
plastic bags, and stored at  $-20 \text{ }^\circ\text{C}$  until their use. Epidermis 326  
sheets were obtained through mechanical separation from the 327  
remaining tissue with forceps, after skin immersion in water at 328  
 $60 \pm 1 \text{ }^\circ\text{C}$  for 1 min. Prior to use for the experiment, the 329  
integrity of the skin was evaluated by measuring the electrical 330  
impedance using an Agilent 4263B LCR Meter (Microlease, 331  
Italy).<sup>24</sup> The epidermis sheets were mounted on the lower half 332  
of the Franz diffusion cells with the stratum corneum facing 333  
upward. The upper and lower parts of the cell were sealed with 334  
Parafilm and fastened together with a clamp. Three hundred 335  
microliters of each formulation were loaded into the donor 336  
compartment. For CBD, vaseline oil solution was used as the 337  
control. 338

The receiver compartment was filled with a mixture of 339  
ultrapure water and ethanol (50:50 v/v) under magnetic 340  
stirring at 1500 rpm. The system was kept at  $37 \pm 1 \text{ }^\circ\text{C}$  by 341  
means of a circulating water bath so that the epidermis surface 342  
temperature was at  $32 \pm 1 \text{ }^\circ\text{C}$  throughout the experiment, 343  
which was carried out in non-occlusive conditions. At fixed 344  
time intervals (i.e., 1, 3, 5, 7, and 24 h) 200  $\mu\text{L}$  of receiver 345  
phase was withdrawn and replaced with an equal volume of 346  
fresh medium. The cumulative amount permeated through the 347  
skin per unit area ( $Q_i$ ) was calculated from the drug 348  
concentration in the receiving medium and plotted as a 349  
function of time. The maximal flux ( $J_{\text{max}}$ ) was determined as 350  
the slope of the linear portion of the plot  $Q_i$  versus time. 351

**2.7. Statistical Analysis.** The differences of the perform- 352  
ance of the formulations in study were evaluated by analysis of 353  
the variance followed by Tukey post hoc analyses (OriginPro 354  
2021b). The level of significance was taken as  $p < 0.05$ . 355

### 3. RESULTS AND DISCUSSION

**3.1. Characterization of Proliposomal Powders.** In the 356  
attempt to prepare proliposomes by spray-drying, the use of 357  
co-solutions was preferred to the suspensions due to issues 358  
related to the clogging of the tubing and nozzle. In particular, 359  
the use of sucrose and a methanol/water solution in 3.4:1 ratio 360  
allowed the preparation of physically stable feeds with a total 361  
solid content of 12% w/v. 362

Regarding the ratio between s-PC and sucrose, the process 363  
yield increased with the sucrose content because the carrier 364  
limited the lipid adherence to the glass wall of the drying 365  
chamber. Indeed, the yield was improved from about 60% to 366  
about 90% for s-PC/sucrose ratio 1:1 and 1:3, respectively. 367  
The moisture content of the spray-dried powders ranged 368  
between 2 and 4%. Proliposomes had a diameter smaller than 369  
10  $\mu\text{m}$  (Figure 1) and, consequently, the powder did not 370  
satisfy the flowability test. 371

In the case of the slurry method, mixtures at the lowest s- 372  
PC/sugar ratio led to wax-like and unprocessable materials. 373  
Moreover, only trehalose provided suitable powders with a 374  
mean diameter of about 330  $\mu\text{m}$  (Figure 1). Even if the 375  
moisture content was about 10% due to trehalose's 376  
hygroscopicity, the powders obtained showed an angle of 377  
repose of  $36 \pm 3^\circ$  and a compressibility index,  $I_c = 23.5$ , 378  
showing an acceptable flowability according to European 379  
Pharmacopeia specifications. It should also be mentioned that 380  
the good flowability of proliposomes prepared by slurry 381  
method is desirable since powders should be poured in the 382  
mixing vessel through a hopper. 383

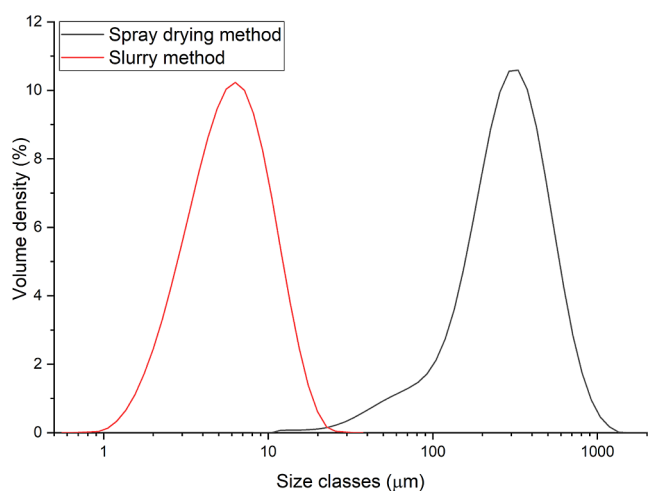


**Figure 1.** Granulometry of proliposomes at 1:2 sPC-sugar ratio obtained by spray-drying and slurry method. As an example, the distribution of the powders is reported in both cases.

384 Interestingly, both drying methods did not cause phospho-  
 385 lipid oxidation since no significant variations of the oxidation  
 386 index ( $0.18 < R_{A233/A215} < 0.22$ ) were observed with respect to  
 387 raw s-PC ( $R_{A233/A215} = 0.19 \pm 0.01$ ).

388 Proliposomes with a lipid/sugar ratio of 1:3 were discarded  
 389 because of the tackiness of the obtained powders that affect the  
 390 handling of the intermediate product. Since the surface area of  
 391 the powder and the type of sugar may be critical for the  
 392 formation of unilamellar liposomes with a narrow polydispersity  
 393 index, all proliposomes were used for the further studies  
 394 independently of their physical features.

395 **3.2. Physico-Chemical Characterization of DiMiL**  
 396 **Systems.** The hydration of proliposomes with micelle  
 397 dispersion allowed to obtain a monodisperse population of  
 398 liposomes with the desired size (Table 1).

399 The presence of the sugar in the aqueous core of liposomes,  
 400 as a result of the hydration process (not removable by  
 401 purification), affected neither the encapsulation efficiency of  
 402 CBD nor the deformability of the DiMiL systems which were  
 403 comparable to those obtained in liposomes prepared by  
 404 conventional thin lipid film hydration method (Table 1). The  
 405 deformability of DiMiL systems was high<sup>16</sup> and seemed to  
 406 slightly decrease upon CBD loading. This variation could be

407 attributed to a partial fusion of CBD carrying micelles into the  
 408 external bilayer. In agreement with SAXS data detailed below,  
 409 it might be supposed that a fraction of the loaded CBD enters  
 410 in the bilayer and modifies the fluidity of the membrane. In  
 411 fact, thermal behavior of a model membrane made of 1,2-  
 412 dipalmitoyl-*sn*-glycero-3-phosphocholine (DPPC) significantly  
 413 changed in presence of CBD since after drug encapsulation the  
 414 main transition temperature of DPPC shifted from  $42.2 \pm 0.1$   
 415 to  $37.3 \pm 0.5$  °C with a concomitant reduction of the  
 416 transition enthalpy from  $37.0 \pm 0.5$  to  $16.3 \pm 1.0$  J/g. These  
 417 results confirm the fluidizing effect exerted by CBD, already  
 418 verified in a previous work.<sup>23</sup> The positive effect of CBD on  
 419 the  $k$  value was not evidenced for the FH4 pair. This behavior  
 420 might be justified considering the lower  $k$  value registered for  
 421 the placebo formulation, FH4, and again in light of the results  
 422 of the SAXS analyses that evidenced a greater presence of  
 423 surfactant-based micelles in the bilayer for FH4 with respect to  
 424 FH10 DiMiL systems, which can contribute to the overall  
 425 fluidity of the membrane.

426 **3.3. Structural Analysis of DiMiL Systems.** Cryo-EM  
 427 clearly evidenced the micelles-in-liposomes structure of DiMiL  
 428 systems (Figure 2). Micelles were found in the aqueous core of  
 429 both FH4 and FH10 liposomes. However, in the case of FH4,  
 430 micelles were not uniformly distributed and empty liposomes  
 431 coexist with liposomes encapsulating a variable number of  
 432 micelles (Figure 2B). Increasing the concentration of micelles  
 433 in FH10, micelles were uniformly present in the core of  
 434 analyzed DiMiL systems (Figure 2C). Moreover, the mean  
 435 diameter of micelles was in agreement with DLS data ( $d: 12 \pm$   
 436  $0$  nm; PDI:  $0.06 \pm 0.00$ ). Finally, no trace of micelles was  
 437 revealed in the dispersing medium suggesting the stability of  
 438 the formed system after preparation.

439 The structure of the liposomes at the nanoscale was  
 440 deepened by SAXS experiments. The comparison among  
 441 SAXS spectra of conventional deformable liposomes (FH0,  
 442 without micelle in the inner core), FH4 and FH10 is reported  
 443 in Figure S1. While the similarities in the overall features of the  
 444 intensity profiles confirm the liposomal structure of FH4 and  
 445 FH10, DiMiL systems are clearly distinguishable from the  
 446 conventional liposomes (FH0). The low and medium  $q$   
 447 behavior of the curves indicates a slightly smaller radius of the  
 448 liposomes in the presence of micelles (from about 120 to 100  
 449 nm) and a different contrast profile of the bilayer. This latter

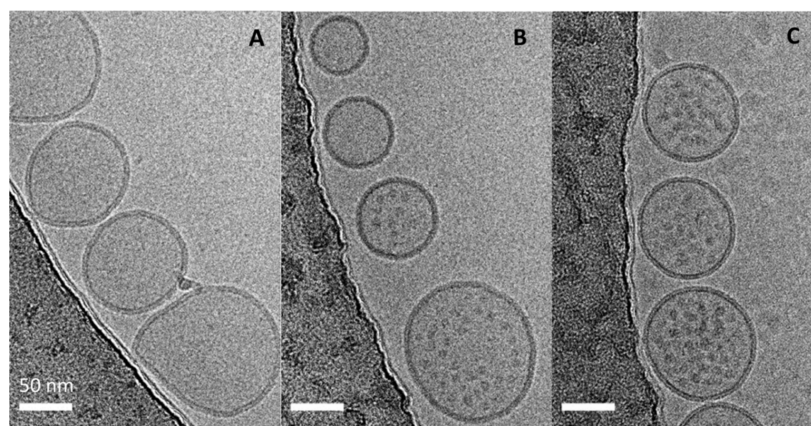


**Figure 2.** Cryo-EM of (a) conventional deformable liposomes, FH0; (b) DiMiL at 4% micelles concentration, FH4; and (c) DiMiL at 10% micelles concentration, FH10.

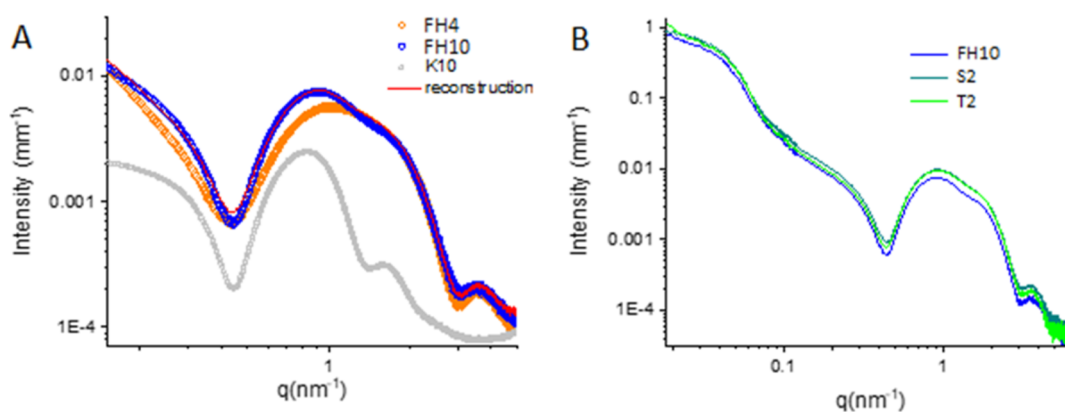


**Figure 3.** Effect of micelle and sugars on SAXS spectra of placebo formulations. Panel A: FH10 experimental spectrum (blue dots) and the reconstruction (red line) obtained by summing a proper fraction (0.15) of 10% Kolliphor micellar dispersion spectrum (K10, gray points) to the FH4 spectrum (orange diamonds). Panel B: spectra recorded on S2 (dark green) and T2 (light green) which evidence the lack of contribution of trehalose and sucrose, respectively.

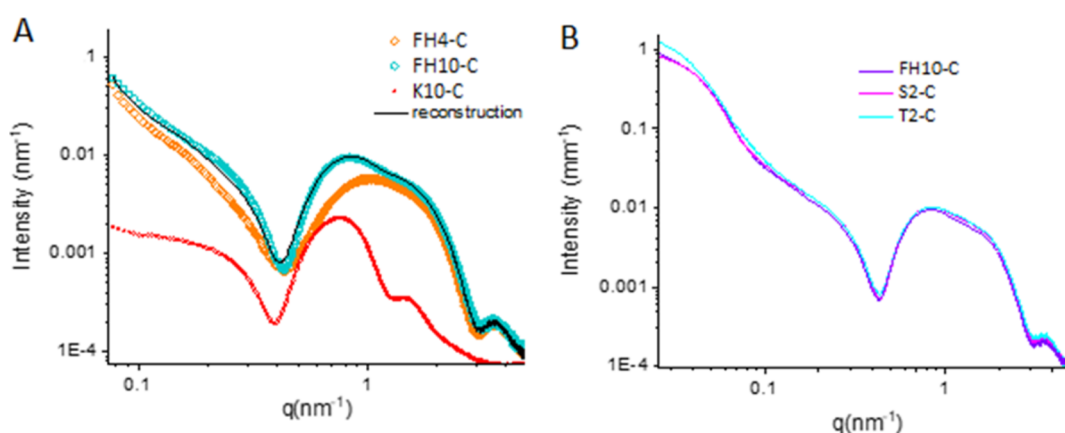


**Figure 4.** Effect of sugars on SAXS spectra of CBD-loaded formulations. Panel A: FH10-C experimental spectrum (light blue dots) and the reconstruction (black line) obtained by summing a proper fraction (0.17) of the CBD micellar dispersion spectrum (K10 CBD, red points) to the FH4-C spectrum (orange diamonds). Panel B: spectra recorded on T2-C (light blue) and S2-C (magenta) which confirm the evidence of the lack of contribution of trehalose and sucrose, respectively.

450 feature suggests a partial insertion of Kolliphor molecules in  
451 the bilayer of the liposomes.

452 The presence of micelles in the purified DiMiL was verified  
453 by SAXS spectra reconstruction.

454 The SAXS spectra of placebo formulations FH4 and FH10  
455 are reported in Figure 3A along with the 10% w/v Kolliphor  
456 micellar dispersion (K10). The structural characterization of  
457 Kolliphor micelles at different concentrations is reported in  
458 Figure S2. As observed before, the intensity profiles of DiMiL  
459 systems were different from those of conventional liposomes  
460 (Figure S1), reinforcing the hypothesis of the partial insertion  
461 of some Kolliphor molecules in the bilayer, independently of  
462 the micelle concentration of the hydration medium. Moreover,  
463 an undulation is visible at  $q \sim 0.85 \text{ nm}^{-1}$  in FH10 spectrum  
464 (Figure 3A, blue dots), being almost undetectable in the case  
465 of FH4. This intensity broad maximum is at the same  $q$   
466 position as the one observed in the spectrum of Kolliphor  
467 micelles (Figure 3A, gray squares). An excellent reconstruction  
468 of the FH10 intensity profile was obtained by summing a  
469 proper fraction of the spectrum of 10% Kolliphor micellar  
470 dispersion (0.15) to the FH4 spectrum, as reported in Figure  
471 3A, red line. The fraction of the micellar spectrum and the  
472 internal aqueous volume of liposomes (size 100–120 nm) are  
473 comparable, as calculated for a 30 mg/mL concentration of

lipid components used in this work. This result indicates that  
474 micelles are homogeneously distributed in all liposomes.  
475 Notably, a good reconstruction cannot be obtained by  
476 summing an intensity contribution of Kolliphor micelles at  
477 lower concentration (2.5–4% w/v), whose spectra differ from  
478 that of Kolliphor at 10 and 4 w/v %, as discussed in the  
479 Supporting Information section (Figure S2). This result reveals  
480 that Kolliphor micelles in the core of FH10 are close to  
481 theoretical value. These data were in agreement with the cryo-  
482 EM results that showed a higher number of micelles in the core  
483 of FH10 with respect to FH4.  
484

The encapsulation of CBD in the systems did not affect their  
485 key structural properties. Figure 4A reports the spectrum of  
486 CBD-loaded Kolliphor micelles and the spectra of CBD-loaded  
487 DiMiL systems (the comparison with unloaded systems,  
488 micelles, and placebo DiMiL, are reported in Figures S3 and  
489 S4). The FH10-C reconstruction has been obtained by  
490 summing the intensity contribution of CBD-loaded micelles  
491 (0.17) to the FH4 spectrum, similarly to the unloaded system.  
492 Results show that DiMiL peculiar micelles in liposomes  
493 structure is preserved in the presence of CBD: the bilayer of  
494 the liposomes contains Kolliphor and possibly CBD, while the  
495 core contains stable micelles, which in the case of FH10-C are  
496 uniformly distributed at a concentration of about 10%.  
497

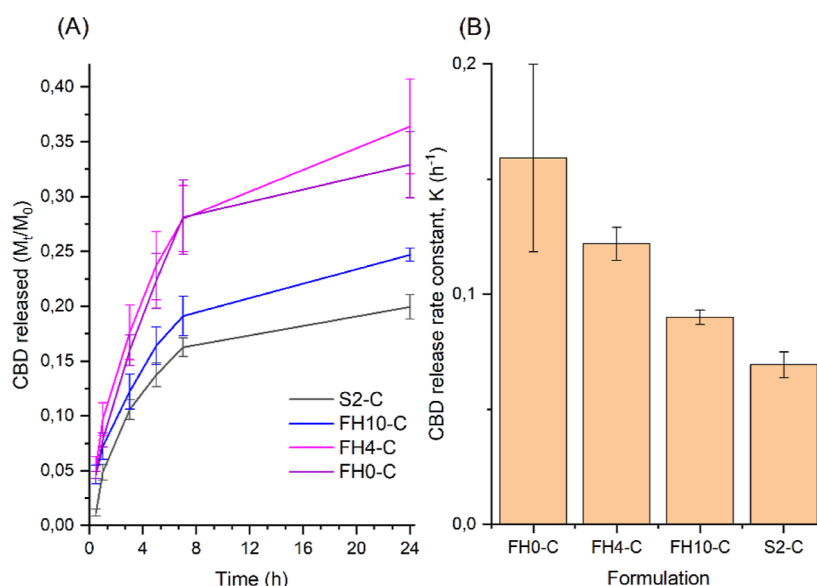


**Figure 5.** In vitro CBD release profiles of DiMiLs at different Kolliphor concentrations (hydrated without micelles, FH0-C; 4% w/v, FH4-C; 10% w/v FH10-C) against deformable liposomes prepared by hydration of proliposomes made of sucrose (S2-C). Panel A: the CBD release profiles; Panel B: release rate constants calculated in the 30 min–7 h range.

**Table 2.** Effect of Surfactants on the Main Transitions of DPPC Bilayers ( $n = 3$ )

formulation	peak 1 pre-transition <sup>a</sup>		peak 2 main phase transition		peak 3	
	$T_p$ (°C)	$T_m$ (°C)	enthalpy (J/g)	$T$ (°C)	enthalpy (J/g)	
DPPC	39.93 ± 0.11	42.2 ± 0.07	37.0 ± 0.5			
DPPC/T80	32.16 ± 0.13	41.6 ± 0.01	28.5 ± 0.4			
DiMiL (4)	31.42 ± 0.65	40.2 ± 0.08	9.9 ± 1.2			
DiMiL (10)	32.33 ± 0.90	39.8 ± 0.04	6.3 ± 0.9	46.0 ± 0.02	1.6 ± 0.1	

<sup>a</sup>Inflection point.

498 Moreover, the additional presence of sugars did not affect  
499 the DiMiL systems since the intensity spectra in Figure 4A,B  
500 displayed an identical profile, the shift in intensity being  
501 ascribable to a small contrast variation due to sugars. Results  
502 excluded any structural modifications in the presence of sugars  
503 for both unloaded and CBD-loaded DiMiLs.

504 **3.4. In Vitro Drug Release.** The release rate constant of  
505 CBD from the micellar dispersions was about 0.25 h<sup>-1</sup>  
506 independent of Kolliphor concentration (4% or 10% w/v)<sup>1</sup>  
507 and the amount of CBD diffused through the membrane after  
508 5 h was up to 40%. This value was twice with respect to those  
509 measured on the DiMiL system, confirming that the  
510 encapsulation of CBD-loaded micelles in the inner core of  
511 the liposomes assures a better control of the drug release.

512 The release rate constants FH10-C and S2-C were  
513 significantly lower ( $p < 0.05$ ) with respect to those of both  
514 conventional deformable liposomes (FH0-C) and FH4-C,  
515 regardless of the preparation method (Figure 5). In contrast,  
516 the release rate of FH4-C was not different from that of  
517 conventional deformable liposomes. These data confirm the  
518 SAXS evidence on the insertion of Kolliphor and CBD  
519 molecules in the liposome bilayer, leading to a prevalent  
520 distribution of the drug in the bilayer rather than in the  
521 aqueous core of liposomes.

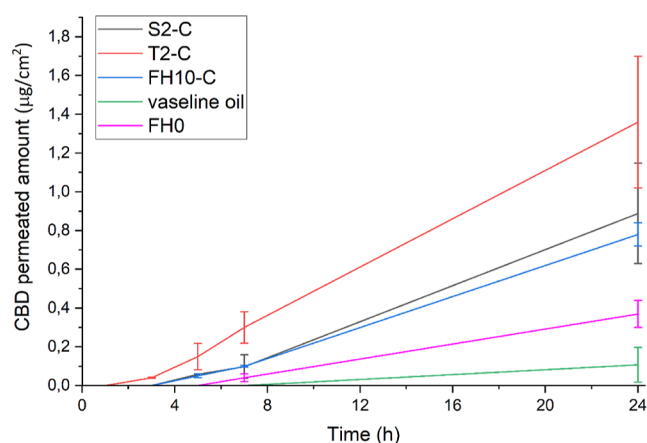
522 At higher micellar concentration, a threshold might be  
523 reached, above which micelles as a whole could fuse with the  
524 bilayer forming Kolliphor-rich domains in the liposome bilayer.  
525 To verify this hypothesis, the thermotropic behavior of

liposome bilayers in the presence of 4 and 10% micelles was  
studied by DSC. For the thermal analyses, s-PC was replaced  
by DPPC because the low transition temperature,  $T_m$ , at about  
–20 °C would have made the analysis difficult. As summarized  
in Table 2, DPPC bilayers showed the characteristic thermo-  
gram consisting of enthalpy event corresponding to the pre-  
transition temperature,  $T_p$ , at 39.93 ± 0.11 °C and a sharp  
endothermic event, namely, the main transition temperature,  
 $T_m$ , at 42.2 ± 0.07 °C. The addition of 15% T80 to the bilayer  
led to a shift of both  $T_p$  and  $T_m$  toward lower values (Table 2).  
At the concentration of T80 used in the study, the shape of  
the peak of the main transition did not change, whereas the  
enthalpy slightly decreased. These data are in agreement with  
those reported in literature, confirming the insertion of T80  
within the lipid bilayer with an overall fluidizing effect, but  
without the formation of new species.<sup>25</sup>

The hydration of DPPC-T80 bilayers with a 4% Kolliphor  
dispersion (DiMiL 4) caused a more pronounced depression  
of the  $T_m$  peak that shifted to 40 °C and became very broad  
and with a very low enthalpy. This pattern suggests that the  
fusion of micelles with the bilayer, leads to a further  
fluidification of the membrane, as evidenced in the  
deformability test. At higher Kolliphor concentrations (i.e.,  
10% w/v),  $T_m$  did not undergo to further decrease confirming  
the saturation of the Kolliphor solubilization within the  
liposome bilayer. Surprisingly, a third endothermic event  
centered at about 46 °C was evident in the DSC traces (Table  
2). This event at  $T > T_m$  may be ascribed to a phase separation

554 within the membrane with the formation of regions where lipid  
555 chains are more rigid and resistant to a transition, as could  
556 occur in the case of interdigitated lipid chains.<sup>26–28</sup> The  
557 simultaneous presence in the bilayer of mixed lipid/surfactant  
558 islands and rigid regions, may improve the stability of the  
559 DiMiL system despite the high content of surfactants.

560 **3.5. In Vitro Skin Permeability Studies.** The main  
561 limitation in CBD permeation study is related to the poor drug  
562 solubility; therefore, a solution of CBD in vaseline oil was used  
563 as control. The encapsulation of the drug in the DiMiL system  
564 improved the in vitro skin permeation of CBD with respect to  
565 both control solution and conventional deformable liposomes  
566 (FH0-C), as already demonstrated with other drugs.<sup>14</sup>  
567 Moreover, DiMiL increased the CBD permeation flux of  
568 about 5 and 3 times with respect to solution and FH0-C,  
569 respectively. Furthermore, the lag time was significantly  
570 shortened since FH10-C and S2-C allowed the detection and  
571 quantification of the drug in the receiver solution already after  
572 3 and 5 h, respectively (Figure 6). Interestingly, it was



573 **Figure 6.** Skin permeation profile through human epidermis of CBD  
574 delivered by DiMiL deriving from hydration of proliposomes obtained  
575 by spray-drying (S2-C) and slurry method (T2-C) or DiMiL prepared  
576 by conventional thin lipid film hydration method (FH10-C). Vaseline  
577 oil and liposomes without micelles (FH0) were used as controls.

578 observed that the type of sugar used for the preparation of  
579 proliposomes had a role in defining the skin permeation  
580 properties of the system since the presence of residual  
581 trehalose in the formulation T2-C resulted in a significant  
582 improvement of CBD permeation (lower lag time and  
583 increased permeated amounts) with respect to FH10-C and  
584 S2-C (Figure 6). These data can be justified in light of the  
585 recent findings of Greco and co-workers<sup>15</sup> who suggested that  
586 the addition of trehalose to cream products increases the skin  
587 hydration levels and significantly decreases the mean basal  
588 values of transepidermal water loss (TEWL).<sup>18</sup> As a  
589 consequence, the improvement in skin hydration may cause  
590 an enlargement of the hydrophilic pores of the stratum  
591 corneum favoring the drug diffusion. This aspect is particularly  
592 interesting considering the final therapeutic indication of the  
593 topical preparation of CBD, namely as anti-inflammatory drug  
594 for which the onset of action is a key parameter.<sup>29</sup> Finally, it is  
595 also important to remark that CBD has a very strong affinity  
596 for stratum corneum lipids, mainly ceramides; therefore, it has  
597 a very poor tendency to diffuse toward the viable epidermis.<sup>30</sup>  
598 Instead, the amount of CBD found in the stratum corneum at  
599 the end of the in vitro permeability studies was almost 10-fold

600 lower after application of DiMiL systems than vaseline oil (S2-  
601 C:  $4.67 \pm 1.23 \mu\text{g}/\text{cm}^2$ ; vaseline oil:  $39.13 \pm 6.81 \mu\text{g}/\text{cm}^2$ ),  
602 confirming the potentiality of DiMiL as drug carrier for the  
603 skin delivery of poorly permeable compounds.

#### 604 4. CONCLUSIONS

605 The use of proliposomes as carriers for (trans)dermal delivery  
606 has been scantily investigated. Consequently, there is a lack of  
607 information about the effect of the preparation process and  
608 excipient choice on the quality attributes of the final system. In  
609 this work, it was made an attempt to deepen these aspects  
610 focusing on the selection of sugar carriers as function of the  
611 preparation method and their effect on the structure and  
612 functionality of deformable liposomes.

613 Among the preparation methods tested, spray-drying  
614 resulted more versatile since it allowed to obtain suitable  
615 proliposomal powders also using the lowest sugar/lipid ratio  
616 (1:1), even if the resulting powders were unable to flow. The  
617 slurry method instead required higher amounts of carrier (2:1/  
618 3:1 sugar/s-PC ratio) and gave free-flowing powders only  
619 using trehalose as a carrier.

620 It is worth noting that both selected sugars (sucrose and  
621 trehalose) did not affect the structure of deformable liposomes  
622 as supported by SAXS data. This was unexpected since it is  
623 well known that disaccharides as sucrose and trehalose strongly  
624 interact with the polar heads of the phospholipids. This  
625 interaction is generally exploited to stabilize the structure of  
626 liposomes, for example, during freeze-drying. Nevertheless,  
627 according to our experimental data, this stabilization does not  
628 cause a loss of deformability of the carrier, which could in turn  
629 affect the skin penetration behavior. The latter seemed instead  
630 to be affected by the nature of the sugar used during  
631 proliposomes preparation. In fact, it was found that the  
632 addition of trehalose led to an improvement of the permeation  
633 flux of CBD as result of the increase of skin hydration level,  
634 even if further data are required to confirm this suggestion.

635 Finally, in this work, the internal structure of the recently  
636 proposed DiMiL carrier was deepened. Information provided  
637 by cryo-EM and SAXS analyses not only confirmed the  
638 micelles-in-liposomes structure but evidenced for the first time  
639 the key role of the Kolliphor concentration in defining the final  
640 organization of the DiMiL system. In fact, it was definitively  
641 proven that 10% w/v Kolliphor concentration guarantees a  
642 complete and homogeneous distribution of micelles in the  
643 inner core of all vesicles of DiMiL systems and an enough  
644 stable membrane to assure a controlled drug release rate. More  
645 in general, deep experimental characterization provides useful  
646 information about the structure of deformable liposomes,  
647 highlighting, as for DiMiL, that a change in the manufacturing  
648 process does not always imply a significant modification in the  
649 structure and function of liposomes. These structural studies  
650 may represent then a helpful tool to rationalize the design of  
651 the production process and to define the formulation space of  
652 liposomal based products to be applied on the skin.

#### 653 ■ ASSOCIATED CONTENT

##### 654 Supporting Information

655 The Supporting Information is available free of charge at  
656 <https://pubs.acs.org/doi/10.1021/acs.molpharmaceut.3c00044>.

657 SAXS data; spectra of conventional liposomes prepared  
658 by the film hydration method, FH4 and FH10; Kolliphor



654 micelles at different concentrations; Kolliphor micelles  
655 blank and encapsulating CBD; and FH10 and FH10-C  
656 systems (PDF)

## 657 ■ AUTHOR INFORMATION

### 658 Corresponding Author

659 Silvia Franzè – Department of Pharmaceutical Sciences,  
660 University of Milan, Milan 20133, Italy; [orcid.org/0000-0003-2231-031X](https://orcid.org/0000-0003-2231-031X); Phone: +39 02 503 24638;  
661 [Email: silvia.franze@unimi.it](mailto:silvia.franze@unimi.it)  
662

### 663 Authors

664 Caterina Ricci – Department of Medical Biotechnology and  
665 Translational Medicine, University of Milan, Segrate 20090,  
666 Italy

667 Elena Del Favero – Department of Medical Biotechnology and  
668 Translational Medicine, University of Milan, Segrate 20090,  
669 Italy; [orcid.org/0000-0002-6584-1869](https://orcid.org/0000-0002-6584-1869)

670 Francesco Rama – Department of Pharmaceutical Sciences,  
671 University of Milan, Milan 20133, Italy

672 Antonella Casiraghi – Department of Pharmaceutical  
673 Sciences, University of Milan, Milan 20133, Italy

674 Francesco Cilurzo – Department of Pharmaceutical Sciences,  
675 University of Milan, Milan 20133, Italy; [orcid.org/0000-0003-3560-291X](https://orcid.org/0000-0003-3560-291X)  
676

677 Complete contact information is available at:

678 <https://pubs.acs.org/10.1021/acs.molpharmaceut.3c00044>

### 679 Notes

680 The authors declare no competing financial interest.

## 681 ■ ACKNOWLEDGMENTS

682 Authors thank ESRF for financial support and beamtime  
683 (DOI: 10.15151/ESRF-ES-585935736) and ID02 staff for  
684 technical support. E.D.F. thanks BIOMETRA Dept. for partial  
685 support (PSR2021\_DEL\_FAVERO). This work benefited  
686 from the use of the SasView application. The cryo-EM  
687 experiments were carried out at the NoLimits center of the  
688 University of Milan.

## 689 ■ REFERENCES

690 (1) Wiedersberg, S.; Guy, R. H. Transdermal drug delivery: 30+  
691 years of war and still fighting. *J. Controlled Release* **2014**, *190*, 150–  
692 156.  
693 (2) Ogunsola, O. A.; Kraeling, M. E.; Zhong, S.; Pochan, D. J.;  
694 Bronaugh, R. L.; Raghavan, S. R. Structural analysis of “flexible”  
695 liposome formulations: new insights into the skin-penetrating ability  
696 of soft nanostructures. *Soft Matter* **2012**, *8*, 10226–10232.  
697 (3) Cevc, G.; Gebauer, D.; Stieber, J.; Schätzlein, A.; Blume, G.  
698 Ultraflexible vesicles, Transfersomes, have an extremely low pore  
699 penetration resistance and transport therapeutic amounts of insulin  
700 across the intact mammalian skin. *Biochim. Biophys.* **1998**, *1368*, 201–  
701 215.  
702 (4) Lai, F.; Caddeo, C.; Manca, M.; Manconi, M.; Sinico, C.; Fadda,  
703 A. What’s new in the field of phospholipid vesicular nanocarriers for  
704 skin drug delivery. *Int. J. Pharm.* **2020**, *583*, 119398.  
705 (5) Benson, H. A. E. Elastic Liposomes for Topical and Transdermal  
706 Drug Delivery. *Curr. Drug Delivery* **2009**, *6*, 217–226.  
707 (6) Souto, E. B.; Macedo, A. S.; Dias-Ferreira, J.; Cano, A.; Zielińska,  
708 A.; Matos, C. M. Elastic and Ultradeformable Liposomes for  
709 Transdermal Delivery of Active Pharmaceutical Ingredients (APIs).  
710 *Int. J. Mol. Sci.* **2021**, *22*, 9743.

(7) Chen, J.; Lu, W. L.; Gu, W.; Lu, S. S.; Chen, Z. P.; Cai, B. C. 711  
Skin permeation behavior of elastic liposomes: role of formulation 712  
ingredients. *Expet Opin. Drug Deliv.* **2013**, *10*, 845–856. 713  
(8) Singh, N.; Kushwaha, P.; Ahmad, U.; Abdullah, M. 714  
Proliposomes: An Approach for the Development of Stable Liposome. 715  
*Ars. Pharm* **2019**, *60*, 231–240. 716  
(9) Hwang, B.-Y.; Jung, B.-H.; Chung, J.-J.; Lee, M.-H.; Shim, C.-K. 717  
In vitro skin permeation of nicotine from proliposomes. *J. Controlled* 718  
*Release* **1997**, *49*, 177–184. 719  
(10) Jukanti, R.; Sheela, S.; Bandari, S.; Veerareddy, P. R. Enhanced 720  
Bioavailability of Exemestane Via Proliposomes based Transdermal 721  
Delivery. *J. Pharm. Sci.* **2011**, *100*, 3208–3222. 722  
(11) AbouSamra, M. M.; Salama, A. H. Enhancement of the topical 723  
tolnaftate delivery for the treatment of tinea pedis via provesicular gel 724  
systems. *J. Liposome Res.* **2017**, *27*, 324–334. 725  
(12) Maniyar, M. G.; Kokare, C. R. Formulation and evaluation of 726  
spray dried liposomes of lopinavir for topical application. *J. Pharm.* 727  
*Invest.* **2019**, *49*, 259–270. 728  
(13) Khan, S.; Madni, A.; Rahim, M.; Shah, H.; Jabar, A.; Khan, M.; 729  
Khan, A.; Jan, N.; Mahmood, M. Enhanced in vitro release and 730  
permeability of glibenclamide by proliposomes: Development, 731  
characterization and histopathological evaluation. *J. Drug Deliv. Sci.* 732  
*Technol.* **2021**, *63*, 102450. 733  
(14) Franzè, S.; Musazzi, U. M.; Minghetti, P.; Cilurzo, F. Drug-in- 734  
micelles-in-liposomes (DiMiL) systems as a novel approach to 735  
prevent drug leakage from deformable liposomes. *Eur. J. Pharm. Sci.* 736  
**2019**, *130*, 27–35. 737  
(15) Greco, L.; Ullo, S.; Rigano, L.; Fontana, M.; Berardesca, E.; 738  
Cameli, N. Evaluation of the Filming and Protective Properties of a 739  
New Trehalose and Ceramides Based Ingredient. *Cosmetics* **2019**, *6*, 740  
62–72. 741  
(16) Parmar, G.; Bala, R.; Seth, N.; Banerjee, A. Proliposomes: novel 742  
drug delivery system. *World J. Pharmaceut. Res.* **2015**, *4*, 679–692. 743  
(17) Khan, L.; Yousaf, S.; Subramanian, S.; Korale, O.; Alhnan, M. 744  
A.; Ahmed, W.; Taylor, K. M.; Elhissi, A. Proliposome powders 745  
prepared using a slurry method for the generation of beclometasone 746  
dipropionate liposomes. *Int. J. Pharm.* **2015**, *496*, 342–350. 747  
(18) Scheau, C.; Badarau, I. A.; Mihai, L.; Scheau, A.; Costache, D. 748  
O.; Constantin, C.; Calina, D.; Caruntu, C.; Costache, R. S.; Caruntu, 749  
A. Cannabinoids in the Pathophysiology of Skin Inflammation. *750*  
*Molecules* **2020**, *25*, 652. 751  
(19) Junaid, M.; Tijani, A. O.; Puri, A.; Banga, A. In vitro 752  
percutaneous absorption studies of cannabidiol using human skin: 753  
Exploring the effect of drug concentration, chemical enhancers, and 754  
essential oils. *Int. J. Pharm.* **2022**, *616*, 121540. 755  
(20) Goldbach, P.; Brochart, H.; Stamm, A. Spray-Drying of 756  
liposomes for a Pulmonary Administration. I. Chemical Stability of 757  
Phospholipids. *Drug Dev. Ind. Pharm.* **1993**, *19*, 2611–2622. 758  
(21) Franzè, S.; Marengo, A.; Stella, B.; Minghetti, P.; Arpicco, S.; 759  
Cilurzo, F. Hyaluronan-decorated liposomes as drug delivery systems 760  
for cutaneous administration. *Int. J. Pharm.* **2018**, *535*, 333–339. 761  
(22) Franzè, S.; Donadoni, G.; Podestà, A.; Procacci, P.; Orioli, M.; 762  
Carini, M.; Minghetti, P.; Cilurzo, F. Tuning the Extent and Depth of 763  
Penetration of Flexible Liposomes in Human Skin. *Mol. Pharm.* **2017**, 764  
*14*, 1998–2009. 765  
(23) Franzè, S.; Angelo, L.; Casiraghi, A.; Minghetti, P.; Cilurzo, F. 766  
Design of Liposomal Lidocaine/Cannabidiol Fixed Combinations for 767  
Local Neuropathic Pain Treatment. *Pharmaceutics* **2022**, *14*, 1915. 768  
(24) Franzè, S.; Gennari, C. G. M.; Minghetti, P.; Cilurzo, F. 769  
Influence of chemical and structural features of low molecular weight 770  
heparins (LMWHs) on skin penetration. *Int. J. Pharm.* **2015**, *481*, 771  
79–83. 772  
(25) El Maghraby, G. M. M.; Williams, A. C.; Barry, B. Interactions 773  
of surfactants (edge activators) and skin penetration enhancers with 774  
liposomes. *Int. J. Pharm.* **2004**, *276*, 143–161. 775  
(26) Marsh, D. Structural and thermodynamic determinants of 776  
chain-melting transition temperatures for phospholipid and glyco- 777  
lipids membranes. *Biochim. Biophys. Acta Biomembr.* **2010**, *1798*, 40– 778  
51. 779

- 780 (27) Leonenko, Z. V.; Finot, E.; Ma, H.; Dahms, T. E. S.; Cramb, D.  
781 T. Investigation of Temperature-Induced Phase Transitions in DOPC  
782 and DPPC Phospholipid Bilayers Using Temperature-Controlled  
783 Scanning Force Microscopy. *Biophys. J.* **2004**, *86*, 3783–3793.
- 784 (28) Oliveira, T. R.; Duarte, E. L.; Lamy, M.; Vandenbranden, M.;  
785 Ruyschaert, J.; Lonez, C. Temperature-Dependence of Cationic  
786 Lipid Bilayer Intermixing: Possible Role of Interdigitation. *Langmuir*  
787 **2012**, *28*, 4640–4647.
- 788 (29) Hammell, D. C.; Zhang, L. P.; Ma, F.; Abshire, S. M.;  
789 McIlwrath, S. L.; Stinchcomb, A. L.; Westlund, K. N. Transdermal  
790 cannabidiol reduces inflammation and pain-related behaviours in a rat  
791 model of arthritis. *Eur. J. Pain* **2016**, *20*, 936–948.
- 792 (30) Casiraghi, A.; Musazzi, U. M.; Centin, G.; Franzè, S.; Minghetti,  
793 P. Topical Administration of Cannabidiol: Influence of Vehicle-  
794 Related Aspects on Skin Permeation Process. *Pharmaceutics* **2020**,  
795 *13*, 337.